

Noble gas, alkali and alkaline atoms interacting with a gold surface

Grzegorz Lach and Maarten DeKieviet

*Physikalisches Institut der Universität Heidelberg,
Albert-Ueberle-Strasse 3-5, 69120 Heidelberg, Germany*

Ulrich D. Jentschura

*Department of Physics, Missouri University of Science and Technology,
Rolla, Missouri 65409-0640, USA*

The attractive branch of the interaction potentials with the surface of gold have been computed for a large variety of atomic systems: the hydrogen atom, noble gases (He, Ne, Ar, Kr, Xe), alkali atoms (Li, Na, K, Rb, Cs) and alkaline atoms (Be, Mg, Ca, Sr, Ba). The results include highly accurate dynamic polarizabilities for the helium atom calculated using a variational method and explicitly correlated wavefunctions. For other atoms considered we used the data available in the literature. The interaction potentials include both the effects of retardation of the electromagnetic interactions and a realistic representation of the optical response function of gold (beyond the approximation of a perfect conductor). An explicit comparison of our result to the interaction between an atom and a perfect conductor is given.

Keywords: atom-surface interactions; retardation; Van der Waals forces; Casimir forces; quantum reflection; helium; gold; dynamic polarizability

1. Motivation

In the last decade, there has been drastic experimental progress in the field of (ultra-) cold collisions in atomic systems. These may involve interactions among two atoms as well as those between an atom and a solid wall. Among the latter, one of the experimental methods for studying the long range ($z \gg a_0$), attractive part of the interaction potential makes use of the phenomenon of quantum reflection. It was demonstrated, that scattering cold atomic beams under grazing angles from well defined, single crystal solid surfaces is especially useful for probing Casimir-Polder forces. This is due to the fact that quantum reflectivity is particularly sensitive to the shape of the potential, at distances where it is heavily modified by retarda-

tion.¹ Other techniques involving the manipulation of clouds of cold atomic gases, or condensates in the presence of a solid wall² heavily depend on the details of the interaction potential. Despite the abundance of experimental results, the theoretical analysis of the interaction potentials was often based on simple model potentials with parameters chosen to fit the data. Here, we provide accurate atom-surface interaction potentials for the surface of gold based on ab-initio computed atomic dynamic polarizabilities and a compilation of all available optical data in literature.

2. Atom-surface interactions

For distances where the exchange effects become negligible, the atom-surface can be computed by considering a polarizable particle interacting with quantum electromagnetic field fluctuations. In this approach, the solid is treated as a continuous medium having a frequency dependent permittivity $\epsilon(\omega)$. The derivation of the dipolar term $V_1(z)$, dominant at the long-distance limit, has been first performed by Lifshitz,³ and the result when given in atomic units ($m_e = e = \hbar = 1$) reads:

$$V_1(z) = -\frac{\alpha^3}{2\pi} \int_0^\infty d\omega \omega^3 \alpha_1(i\omega) \int_1^\infty d\xi e^{-2\alpha\xi\omega z} H(\xi, \epsilon(i\omega)), \quad (1)$$

where α is the fine structure constant and $\alpha_1(i\omega)$ is the dipole polarizability of the atom [for the fundamental physical constants we take the CODATA⁴ recommended values, e.g., $\alpha = 137.035999679(94)$]. The function $H(\xi, \epsilon)$ is given by:

$$H(\xi, \epsilon) = (1 - 2\xi^2) \frac{\sqrt{\xi^2 + \epsilon - 1} - \epsilon\xi}{\sqrt{\xi^2 + \epsilon - 1} + \epsilon\xi} + \frac{\sqrt{\xi^2 + \epsilon - 1} - \xi}{\sqrt{\xi^2 + \epsilon - 1} + \xi}. \quad (2)$$

This expression simplifies considerably in the limit of a perfect conductor [$\epsilon(\omega) \rightarrow \infty$], for which case the potential becomes:

$$V_1^{(\infty)}(z) = -\frac{1}{4\pi} \int_0^\infty d\omega \alpha_1(i\omega) e^{-2\alpha\omega z} P_1^{(\infty)}(\alpha\omega z), \quad (3)$$

where $P_1^{(\infty)}(z) = 1 + 2z + 2z^2$. Another simplification takes place in the short-distance and long-distance limits. For $z \rightarrow 0$, the interaction potential behaves as:

$$V_1(z) \stackrel{z \rightarrow 0}{\sim} -\frac{1}{4\pi z^3} \int_0^\infty d\omega \alpha_1(i\omega) \frac{\epsilon(i\omega) - 1}{\epsilon(i\omega) + 1} \equiv -\frac{C_3}{z^3}. \quad (4)$$

The long-distance limit the interaction potential for a generic $\epsilon(\omega)$ is:

$$V_1(z) \stackrel{z \rightarrow \infty}{\sim} -\frac{3\alpha_1(0)}{8\pi\alpha z^4} \frac{\epsilon(0) - 1}{\epsilon(0) + 1} \equiv -\frac{C_4}{z^4}. \quad (5)$$

but this result cannot be used for the case of conductors, where ϵ has a pole at $\omega=0$. We have checked that when the $\epsilon(i\omega)$ (a real function) is bounded from below by a/ω , as it is in the case of conductors, the long distance behavior of the potential is equal to the one of perfect conductor, asymptotically parametrized by $C_4^{(\infty)}$:

$$V_1^{\text{cond}}(z) \stackrel{z \rightarrow \infty}{\sim} V_1^{(\infty)}(z) \stackrel{z \rightarrow \infty}{\sim} -\frac{3\alpha_1(0)}{8\pi\alpha z^4} \equiv -\frac{C_4^{(\infty)}}{z^4}. \quad (6)$$

3. Frequency dependent dielectric permittivity of gold

The *ab-initio* computation of the frequency dependent dielectric response function of metals is beyond the reach of present day electronic structure calculations. In this work, the complex frequency dependent permittivity of gold was reconstructed from the experimental optical data. The imaginary part of the dielectric constant was modeled using a function:

$$\text{Im } \epsilon(\omega) = \frac{\omega_p^2 \omega_\tau}{\omega(\omega^2 + \omega_\tau^2)} + \sum_n c_n f_{\text{TL}}(\omega_{0,n}, \omega'_{0,n}, \gamma_n; \omega), \quad (7)$$

where the first term is the Drude model of the free-electron contribution, and the second is a sum of empirical Tauc-Lorentz⁵ functions:

$$f_{\text{TL}}(\omega_0, \omega'_0, \gamma; \omega) = \frac{\omega_0 \gamma (\omega - \omega'_0)^2 \theta(\omega - \omega_0)}{\omega (\omega^2 - \omega_0^2)^2 + \gamma^2 \omega^2}, \quad (8)$$

where $\theta(x)$ is the Heaviside step function [$\theta(x) = 0$ for $x < 0$, and $\theta(x) = 1$ otherwise]. Once a satisfactory representation of the imaginary part of $\epsilon(\omega)$ is found, the real part of the permittivity can be calculated using the Kramers-Kronig relation. The parameters of Eq. (7) have been fitted to the experimental optical data. The data used included the data sets collected in the handbook by Palik⁶ which cover the visible, ultraviolet and X-ray regimes, and various compilations of optical data in the microwave and in the infrared regions of the electromagnetic spectrum.⁷

The results of a global fit of the model (7) to the experimental data for gold are listed (in atomic units) in Table 1 and depicted in Fig 1. Our fitted values of the plasma frequency (ω_p), and the damping frequency (ω_τ) can be compared to the values used by Lambrecht *et al.*⁸ who used values of $\omega_p=0.330$, $\omega_\tau=0.00108$ and $\omega_p=0.276$, $\omega_\tau=0.00478$.

When using the model defined in Eq. (7), we observe a slight, but systematic deviation of the fitted function with respect to the experimental data for the imaginary part of the permittivity in the very low frequency region. In order to improve the fit, we decided to further refine our model

Table 1. Best fit parameters for the analytic model of $\text{Im } \epsilon(\omega)$ for gold according to Eq. (7).

ω_p	0.357091		ω_τ		0.001636		
c_1	3.177115	ω_1	0.117730	ω'_1	0.061100	γ_1	0.114560
c_2	0.483874	ω_2	0.337153	ω'_2	= ω'_1	γ_2	0.262558
c_3	0.106614	ω_3	0.777090	ω'_3	= ω'_1	γ_3	0.140060
c_4	1.988346	ω_4	1.014223	ω'_4	= ω'_1	γ_4	2.017446
c_5	2.220095	ω_5	5.242422	ω'_5	= ω_5	γ_5	10.076456

for the dielectric function by including an additional Drude-model term, corresponding to a conductor with two types of carriers:

$$\text{Im } \epsilon(\omega) = \frac{\omega_{p_1}^2 \omega_{\tau_1}}{\omega(\omega^2 + \omega_{\tau_1}^2)} + \frac{\omega_{p_2}^2 \omega_{\tau_2}}{\omega(\omega^2 + \omega_{\tau_2}^2)} + \sum_n c_n f_{\text{TL}}(\omega_n, \omega'_n, \gamma_n; \omega). \quad (9)$$

The parameter of the model function have been reoptimized using nonlinear least squares fit to the optical data, and their values are presented in Table 2. The double Drude model leads to a significant improvement of the

Table 2. Best fit parameters for the two plasma frequency model of $\text{Im } \epsilon(\omega)$ for gold according to Eq. (9).

ω_{p_1}	0.327756	ω_{τ_1}	0.001127	ω_{p_2}	0.107482	ω_{τ_2}	0.019638
c_1	4.084274	ω_1	0.110273	ω'_1	0.066774	γ_1	0.108472
c_2	0.478826	ω_2	0.337918	ω'_2	= ω'_1	γ_2	0.259896
c_3	0.108575	ω_3	0.776982	ω'_3	= ω'_1	γ_3	0.140290
c_4	2.001595	ω_4	1.011645	ω'_4	= ω'_1	γ_4	2.010662
c_5	2.193675	ω_5	5.168412	ω'_5	= ω_5	γ_5	10.819556

low-frequency behavior of ϵ , but has a negligible influence on the calculated potential. Since there is no physical justification for Eq. (9), we use Eq. (7) for the results obtained in the rest of this paper.

4. Numerical Results

The atom-surface interaction potentials have been computed by numerically evaluating Eq. (1) using Eqs. (7) and (9) and *ab-initio* calculated values of dynamic dipole polarizabilities. For the case of helium the respected polarizabilities have been computed variationally using basis sets of explicitly correlated functions.⁹ For the other atoms considered we used dynamic polarizabilities published by Derevianko, Porsev and Babb.¹⁰

We find it convenient to represent the potential by its short distance

limit multiplied by a “damping function”, accounting for the effects of retardation, which for the dipole case reads:

$$V_1(z) = -\frac{C_3}{z^3} f_3(z) , \quad (10)$$

For the damping function $f_3(z)$, we found the following functional form to lead to an accurate representation of all interaction potential for all atom-wall distances:

$$f_3(z) = \frac{1 + a_1 \alpha z + a_2 (\alpha z)^2}{1 + a_1 \alpha z + b_2 (\alpha z)^2 + b_3 (\alpha z)^3} , \quad (11)$$

with α being the fine structure constant. The equality of the linear terms in both the numerator and in the denominator of this rational function is due to the requirement of the potential having the correct short distance limit: $f_3(z) = 1 + \mathcal{O}[(\alpha z)^2]$. The best values of the parameters a_1 , a_2 , b_2 , b_3 in (11) fitted to the calculated interaction potentials for different atomic species are presented in Tables 3-5, together with the corresponding values of C_3 .

Table 3. Long range potentials for noble gas atoms interacting with a surface of gold. The second row contains the C_3 constants, and the following rows give the values of the $f_3(z)$ damping function, defined in Eq. (10) for different distances. In the last four rows, we present the best fit parameters for the rational function (11) which covers all distances.

	He	Ne	Ar	Kr	Xe
C_3	0.062(3)	0.127(1)	0.415(4)	0.588(5)	0.870(6)
z	$f_3(z) = V(z)/(C_3/z^3)$				
1×10^1	0.99108	0.98804	0.99323	0.99348	0.99405
2×10^1	0.97388	0.96653	0.98014	0.98112	0.98275
5×10^1	0.90949	0.89155	0.92931	0.93352	0.93907
1×10^2	0.80490	0.77796	0.84192	0.85135	0.86320
2×10^2	0.64602	0.61531	0.69933	0.71522	0.73546
5×10^2	0.40337	0.37942	0.45908	0.47873	0.50522
1×10^3	0.25046	0.23481	0.29294	0.30931	0.33232
2×10^3	0.14492	0.13575	0.17185	0.18274	0.19849
5×10^3	0.06539	0.06124	0.07800	0.08322	0.09088
1×10^4	0.03441	0.03222	0.04109	0.04387	0.04796
2×10^4	0.01770	0.01657	0.02114	0.02257	0.02469
5×10^4	0.00721	0.00675	0.00861	0.00919	0.01005
1×10^5	0.00363	0.00339	0.00433	0.00462	0.00506
a_1	4.19366	5.91822	3.76881	3.95140	4.21331
a_2	0.29208	0.47236	0.21430	0.20804	0.20365
b_2	2.13922	3.33497	1.53023	1.47551	1.41033
b_3	0.10861	0.18758	0.06671	0.06066	0.05430

Table 4. Long range potentials for alkali atoms interacting with a surface of gold. The second row contains the C_3 constants, and the following rows give the values of the $f_3(z)$ damping function, defined in Eq. (10) for different distances. In the last four rows, we present the best fit parameters for the rational function (11) which covers all distances.

	Li	Na	K	Rb	Cs
C_3	1.210(5)	1.356(6)	2.058(9)	2.31(1)	2.79(1)
z	$f_3(z) = V(z)/(C_3/z^3)$				
1×10^1	0.99899	0.99845	0.99829	0.99801	0.99780
2×10^1	0.99740	0.99590	0.99542	0.99465	0.99408
5×10^1	0.98992	0.98533	0.98333	0.98086	0.97903
1×10^2	0.97415	0.96515	0.96065	0.95541	0.95169
2×10^2	0.94032	0.92509	0.91803	0.90850	0.90210
5×10^2	0.84866	0.82359	0.82012	0.80456	0.79521
1×10^3	0.73176	0.69946	0.70857	0.69126	0.68309
2×10^3	0.57369	0.53721	0.56295	0.54776	0.54485
5×10^3	0.34082	0.30970	0.34388	0.33492	0.33918
1×10^4	0.19776	0.17688	0.20301	0.19808	0.20323
2×10^4	0.10552	0.09370	0.10926	0.10672	0.11029
5×10^4	0.04353	0.03854	0.04525	0.04422	0.04585
1×10^5	0.02196	0.01943	0.02285	0.02233	0.02318
a_1	6.96178	19.81680	1.50957	1.90225	2.21418
a_2	0.10676	0.30362	2.97205	2.06782	1.55523
b_2	0.44672	1.43152	3.15260	2.30121	1.83158
b_3	0.00659	0.02118	0.15449	0.11044	0.07999

The potentials presented above can be compared to simplified ones used previously¹ in the analysis of the atomic beam experiment measuring the quantum reflectivity. There, retardation has been accounted for using:

$$V(z) = -\frac{C_4}{z^3(z + \lambda)}, \quad (12)$$

in which λ represents the reduced wavelength of the first electronic dipole transition in He, i.e. $\lambda = 178$ Bohr (93\AA). This function has also been used in the preliminary evaluation of the experimental results for ^3He atoms quantum reflecting from a single crystal gold surface. Here however, significant deviations have been found indicating, that the coarse-grained model (12) is not sufficiently complex to mimic the more involved rational structure given in Eqs. (10) and (11).

An independent check of our potentials has been performed by using our model for the dielectric constant $\epsilon(i\omega)$ of gold to calculate the interaction energy between two surfaces of gold, for both semi-infinite solids and for thin foils. Our computations are within 1% of the revisited results of

Table 5. Long range potentials for alkaline atoms interacting with a surface of gold. The second row contains the C_3 constants, and the following rows give the values of the $f_3(z)$ damping function, defined in Eq. (10) for different distances. In the last four rows, we present the best fit parameters for the rational function (11) which covers all distances.

	Be	Mg	Ca	Sr	Ba
C_3	0.650(5)	1.067(6)	1.82(1)	2.19(1)	2.75(1)
z	$f_3(z) = V(z)/(C_3/z^3)$				
1×10^1	0.99797	0.99790	0.99805	0.99788	0.99778
2×10^1	0.99388	0.99394	0.99442	0.99404	0.99382
5×10^1	0.97571	0.97722	0.97909	0.97810	0.97764
1×10^2	0.93887	0.94441	0.94957	0.94792	0.94755
2×10^2	0.86495	0.87903	0.89248	0.89054	0.89129
5×10^2	0.69195	0.72244	0.75855	0.75885	0.76468
1×10^3	0.51642	0.55531	0.61130	0.61588	0.62880
2×10^3	0.34021	0.37699	0.44043	0.44893	0.46827
5×10^3	0.16580	0.18850	0.23484	0.24315	0.26173
1×10^4	0.08878	0.10168	0.12963	0.13511	0.14765
2×10^4	0.04590	0.05270	0.06773	0.07078	0.07784
5×10^4	0.01872	0.02151	0.02772	0.02899	0.03196
1×10^5	0.00942	0.01082	0.01395	0.01460	0.01610
a_1	3.00255	3.88303	12.61180	3.09874	2.83515
a_2	0.12664	0.12802	0.19042	4.88813	2.70340
b_2	0.51498	0.55406	1.27280	5.20283	3.03090
b_3	0.01818	0.01601	0.01848	0.41434	0.20650

Lambrecht *et al.*^{11,12} This gives us confidence, that the ready-to-use interaction potentials for the various atomic species presented in this paper are accurate. In addition, it demonstrates that our simple analytic model of the permittivity of gold may be very useful for future computation of Casimir potential involving gold, for both microscopic and macroscopic bodies.

Acknowledgements

This project was supported by the National Science Foundation (Grant PHY-8555454) and by a precision measurement grant from the National Institute of Standards and Technology. G.L. acknowledges support by the Deutsche Forschungsgemeinschaft (DFG, contract Je285/5-1).

References

1. V. Druzhinina and M. DeKieviet, Phys. Rev. Lett. **91**, 193202 (2003).
2. D. M. Harber, J. M. Obrecht, J. M. McGuirk, and E. A. Cornell, Phys. Rev. A **72**, 033610 (2005).

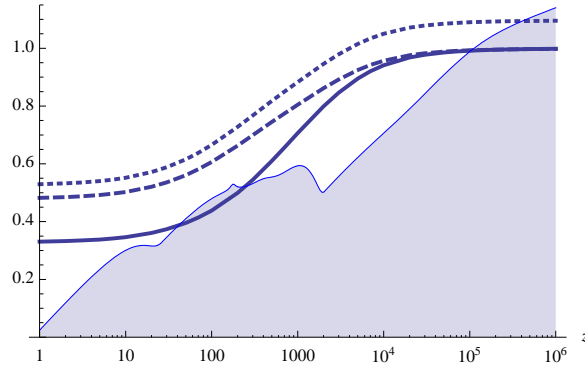


Fig. 1. Ratio between the full He-Au potential $V_1(z)$ calculated using the optical data in (7) and $V_1^{(\infty)}(z)$ (solid curve), between $V_1(z)$ and the approximate model (12) using $C_4 = C_4^{(\infty)}$ (dashed curve) or using the best fit value of $C_4 = 44 \text{ eV}\text{\AA}^4$ (dotted curve). The shaded spectrum in the background depicts $\log \text{Im } \epsilon(\omega)$ of the fit obtained in Table 1, for $\omega = c/z$.

3. E. M. Lifshitz, Zh. Éksp. Teor. Fiz. **29**, 94 (1955), [JETP **2**, 73 (1956)].
4. P. J. Mohr, B. N. Taylor, and D. B. Newell, Rev. Mod. Phys. **80**, 633 (2008).
5. G. E. Jellison, Jr. and F. A. Modine, Appl. Phys. Lett. **69**, 371 (1996).
6. E. D. Palik, *Handbook of Optical Constants of Solids* (Academic Press, San Diego, 1985).
7. H. E. Bennett and J. M. Bennett, *Optical Properties and Electronic Structure of Metals and Alloys edited by F. Abeles* (North-Holland, Amsterdam, 1966); L. G. Schulz, J. Opt. Soc. Am. **44**, 357 and 362 (1954); G. P. Motulevich and A. A. Shubin, Soviet Phys. JETP **20**, 560 (1965); V. G. Padalka and N. Shklyarevskii, Opt. Spectr. USSR **11**, 285 (1961); G. A. Bolotin *et. al.*, Phys. Met. and Mt. **13**, 823 (1962); B. Brändli and A. J. Sievers, Phys. Rev. B **5**, 3550 (1972); J. H. Weaver *et. al.*, *Physics Data, Optical Properties of Metals*, (Fach-Information Zentrum, Karlsruhe, 1981).
8. A. Lambrecht, P. A. Maia Neto and S. Reynaud, New J. Phys. **8**, 243 (2006).
9. G. Lach, B. Jeziorski and K. Szalewicz, Phys. Rev. Lett. **92**, 233001 (2004).
10. A. Derevianko, S. G. Porsev and J. F. Babb, preprint: [arXiv:0902.3929](https://arxiv.org/abs/0902.3929)
11. A. Lambrecht, I. Pirozhenko, L. Duraffourg and Ph. Andreucci. Eur. Phys. Lett. **77**, 44006 (2007).
12. A. Lambrecht, I. Pirozhenko, L. Duraffourg and Ph. Andreucci. Eur. Phys. Lett. **81**, 19901 (2008).